Study on Decay Heat Removal Capability of Reactor Vessel Auxiliary Cooling System

Y. Nishi
I. Kinoshita

Central Research Institute of Electric Power Industry
11-1, Iwatokita, 2-chome
Komae-shi, Tokyo, JAPAN

1. Introduction

The reactor vessel auxiliary cooling system (RVACS) is a simple, passive decay heat removal system for an LMFBR. However, the heat removal capacity of this system is small compared to that of an immersed type of decay heat exchanger. In this study, a high-porosity porous body is proposed to enhance the RVACS's heat transfer performance to improve its applicability.

The objectives of this study are to propose a new method which is able to use thermal radiation effectively, to confirm its heat removal capability and to estimate its applicability limit of RVACS for an LMFBR. Heat transfer tests were conducted in an experimental facility with a 3.5m heat transfer height to evaluate the heat transfer performance of the high-porosity porous body. Using the experimental results, plant transient analyses were performed for a 300MWe pool type LMFBR under a Total Black Out (TBO) condition to confirm the heat removal capability. Furthermore, the relationship between heat removal capability and thermal output of a reactor were evaluated using a simple parameter model.

2. Enhancement of Heat Transfer

A high-porosity porous body is proposed as a heat collector in the annular air flow space to enhance the heat transfer performance of the RVACS. The porous body, made from nickel and chromium, has 92% porosity, a high absorption coefficient, and a low pressure loss. To evaluate the effect of the porous body, heat transfer experiments were performed .

The test facility simulated the annular air flow space between the containment vessel and cavity wall. It consisted of a rectangular duct of 1.2m× 0.4m section and 10m height as shown in Fig. 1. The heated zone was 3.5m high. The maximum heat flux was 30KW/m^2. To obtain a wide range of air velocity, an exhaust fan simulated the stack at the outlet of the test facility. The parameters in these experiments were temperature of the heating wall and the air velocity, both with and without the porous body.

Fig. 2 shows local heat transfer coefficients obtained from these experimental results. In the case without porous body, the heat transfer coefficients at the lower reaches are smaller than those at the upper reaches. But in the case with porous body, the heat transfer coefficients at the lower reaches remain constant or increase slightly than those at the upper reaches.

The Nusselt numbers with porous body are shown in Fig. 3(b), and Fig. 3(a) shows the Nusselt numbers without porous body. It is found that the Nusselt numbers with porous body become greater than those without porous body in all ranges of Reynolds numbers, especially in the high wall temperature condition. The average Nusselt numbers with porous body are about 1.5 to 1.6 times larger than those without porous body.

3. Thermal-hydraulic transient Analysis

3-1. CERES Modeling

The results of the heat transfer experiments were used in the plant transient analyses. The computation code "CERES" was used to predict the temperature profiles and velocity distribution in the plenums, and to evaluate the effectiveness of the RVACS heat removal capability. CERES is a 3D transient calculation code which can evaluate the heat transfer and natural circulation of an LMFBR; it can treat hot plenum, cold plenum, pumps, pipes, IHXs, DHXs, air coolers, and the core. The governing equations treated in CERES modeling are incompressible continuity, Navier-Stokes, and continuity of energy. The flow is solved from pressure fields which are obtained by solving the continuity equations that substituted the Navier-Stokes equation with the SOR or ICCG method. The structure forms in the plenums are expressed by the volume porosity and surface permeability concepts.

3-2. Conditions for Analyses

An LMFBR of 790MWt, shown in fig. 4, a 10.5m diameter reactor vessel and 14.4m high (from bottom of reactor vessel to roof slab), was used as a reference design. A sodium overflow concept was introduced in it during the operation of RVACS. And using the porous body is the reference condition. The properties of the heat transfer associated with RVACS are shown in Table 1. The decay heat curve was provided in tabular data from the ORIGEN code. The flow halving time of the primary pumps were assumed as 10 seconds, and that of secondary pumps were assumed as 5 seconds. The control rods full insertion time was assumed as 2 seconds. The steam generators were assumed to be insulated immediately after scram. The pressure loss coefficient was considered as a function of Reynolds number. The sodium overflow level was assumed as 20cm higher than that of the normal operation level. The RVACS air velocity was assumed to be a constant 7 m/s.

Further analyses were performed to evaluate the effects of the porous body, sodium overflow level and reactor vessel diameter. In these analyses, only one parameter was varied at a time while the other parameters were restrained to their reference design values.

3-3. Results and Discussion

Fig. 5 shows the core decay heat and the heat removal by RVACS and IHXs. The solid line shows the heat removal of the reference case (with porous body), and the dotted line shows the heat removal without porous body. The heat removal with porous body exceeds the decay heat about 19 hours after shutdown, and that without porous body is still less than the decay heat about 20 hours after shutdown. Heat removal by the IHXs decreases instantaneously after RVACS starts.

The sodium flow patterns and the temperature profiles in the hot/cold plenums at steady state, 2 hours, 3 hours and 22 hours after shutdown in the case with porous body are shown in Fig. 6. Fig. 6(b) shows the flow patterns and the temperature profiles just before the start of sodium overflow. At that time the sodium flow rate in the core is maintained via IHXs. After the sodium overflow path is established, the sodium flow rate in the core is maintained via overflow path and the IHXs. The maintained core flow is preserved until 22 hours after shutdown.

The sodium temperatures of core outlet and inlet are shown in Fig. 7. The outlet temperatures increase quickly with decreasing sodium flow rate,

and then decrease when the heat removal by the IHXs is reestablished (as in Fig. 5). The secondary sodium flow rate is small 30 minutes after scram due to decreasing difference of temperature between the steam generators and the IHXs. But 1 hour after shutdown, the average temperature of the hot plenum becomes higher than the secondary sodium, so the flow rate in the IHXs and their heat removal recovered slightly.

The average hot plenum temperature and cold plenum temperature at the two plenum elevations (Z=0.2m, 5.3m) in both the reference and without porous body cases are shown in Fig. 8. The predicted hot plenum peak temperature for the reference case is about 640°C at about 22 hour after shutdown. On the other hand, without the porous body, average hot plenum temperature keeps increasing and reaches 675°C at 24 hours after scram yet.

The effect of reactor vessel diameter on the sodium peak temperature is shown in Fig. 9. An increase in the reactor vessel diameter to 11m (from the reference value of 10.5m) reduced the hot plenum peak temperature by 50°C due to the sodium inventory increase and the larger heat transfer area.

The effect of the overflow level on the sodium peak temperature is shown in fig. 10. A decrease in the overflow level to 10cm (from the reference value of 20cm) did not have a large influence on the peak temperature of the hot plenum. The effect of changing overflow level is small compared to that of reactor diameter.

4. Estimation of RVACS Applicability

To estimate the applicability of RVACS to an LMFBR, a parametric study was performed with a simple parameter model. In this model, the whole system inside the reactor was treated as a well mixed homogeneous mass.

4-1. The Simple Parameter Model

If there is no heat removal except for that by RVACS, the conservation of energy is

$$mCp \frac{dT}{dt} = Q_{decay} - Q_{rvacs}, \tag{1}$$

where

mCp	:	heat capacity of the homogenized primary system
T	:	temperature
Q_{decay}	:	reactor decay power
Q_{rvacs}	:	heat removal via RVACS
t	:	time.

In the RVACS, temperatures change slowly with time, and the system can be treated as being in quasi-steady state. With this approximation, the heat removal from the sodium to the air is described by the following equations:

$$Q_{flux} = 2 \cdot U_{air} \cdot A_{flow} \cdot \rho_{air} \cdot Cp_{air} \cdot (T_{air}ave - T_{air}in), \tag{2}$$

$$Q_{flux} = \frac{\lambda \cdot (T_p - T_{rv})}{dL_{rv}}, \tag{3}$$

$$Q_{flux} = \frac{\lambda \cdot (T_{cv}in - T_{cv}out)}{dL_{cv}}, \tag{4}$$

$$Q_{flux} = \alpha \cdot (T_{cv}out - T_{air}ave), \tag{5}$$

$$Q_{flux} = \frac{\sigma \cdot (T^4_{rv} - T^4_{cv}in)}{\frac{1}{\varepsilon_{rv}} + \frac{1}{\varepsilon_{cv}} - 1}, \tag{6}$$

and

$$Q_{rvacs} = Q_{flux} \cdot A_{heat}. \tag{7}$$

Where

Q_{flux}	:	removal heat flux	ρ	:	density
U_{air}	:	air velocity	Cp	:	specific heat
dL	:	thickness of vessel	λ	:	thermal conductivity
A_{flow}	:	area of air flow path	α	:	heat transfer coefficient
A_{heat}	:	area of heat removal	σ	:	Stefan-Boltzman constant
in	:	inlet/inside	ε	:	emissivity
out	:	outside	rv	:	reactor vessel
ave	:	average	cv	:	containment vessel.

The same heat transfer correlation between the air and the containment vessel as CERES analyses are used in this model (Table 1).

Initially, a comparison of reference results of the CERES code with those of the simple parameter model was performed. In the CERES calculation, the IHXs were insulated immediately after shutdown because of the agreement with the simple model. Fig. 11 shows the comparison of core decay heat with the RVACS heat removal. The dotted line denotes the results of the simple model. It is found that the heat removal rate of RVACS predicted by the simple model is in good agreement with the results of the CERES code.

Fig. 12 shows the predicted temperature with both models. The predicted temperatures by the simple model have intermediate values and temperature changes between the hot and cold sodium similar to those predicted by the CERES code.

4-2. Results and Discussion

The applicability of this type of RVACS was evaluated by using simple parameter model. The heat capacity of the homogenized primary system was assumed to be in proportion to the square of the diameter. Other parameters, such as reactor vessel height, were fixed. The reactor diameter, reactor power, and homogenized heat capacity were changed as a parameter. In this model, the peak critical temperature was set to 600°C because of the temperature difference shown in Fig. 12.

Fig. 13 shows the predicted application limit. The vertical axis denotes the approximate volume of the reactor vessel as defined by the equation:

$$V = \frac{\pi \cdot D^2 \cdot h}{4}, \tag{8}$$

where

V : approximate volume,
D : reactor vessel inner diameter,
h : height from the bottom of reactor vessel to the bottom of roof slab.

The horizontal axis denotes thermal plant power. Fig.13 shows that the RVACS using the porous body concept is suitable for about a 450MWe LMFBR under preconditions. If the IHXs were not insulated, or the air velocity not assumed to be constant value, the applicability range would be greater than that derived in this calculation.

5. Summary

To enhance the heat transfer performance of RVACS, application of a high-porosity porous body is proposed. From the heat transfer experiments, the average Nusselt number with porous body is 1.5 times larger than that without the porous body.

Using the experimental results, the plant transient analysis have been made to evaluate the effect of the porous body on the temperature profiles with CERES code.

This analyses reveal that the porous body has sufficient performance to decrease the hot plenum peak temperature of the reference reactor in the TBO event.

The effects of reactor diameter and overflow level were also evaluated.

The simple parameter model predicted that this type of RVACS is applicable to an LMFBR in the 450MWe range.

REFERENCES

1. Constantine P.TZANOS, Dean R.PEDERSEN, Analysis of RVACS tests for COMMIX validation, Nuclear Engineering and Design 121 (1990) 59-67

2. GREGORY J. Van TUYLE, PETER KROEGER, GREGORY C.SLOVIK, BING C.CHAN, ROBERT J.KENNETT, ARNOLD L.ARONSON, Examining the inherent safety of PRISM, SAFR, and the MHTGR, Nuclear Technology, Vol.91, AUG (1990) 185-202

3. KAMIUTO. K., et al., Experimental and analytical study on enhancement of simultaneous radiative and convective heat transfer by porous bodies with high porosity, J. Nuclear Science and Technology, Vol.17, No.6, (1980) 425

4. KINOSHITA. I., et al., Study of simultaneous conductive and radiative heat transfer in high porosity materials, Proceeding of The Seventh International Heat Transfer Conference, Vol.2, 505-510, (1982)

5. CONSTANTINE P.TZANOS, JACK H.TESSIER, and DEAN R.PEDERSEN, An optimization study for the reactor vessel auxiliary cooling system of a pool liquid-metal reactor, Nuclear Technology Vol.94 APR. 68-79, (1991)

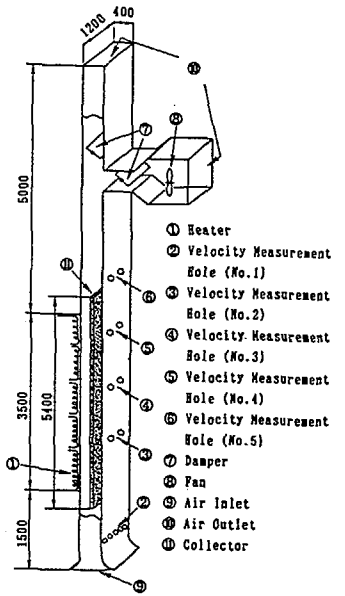

Fig.1 Test facility.

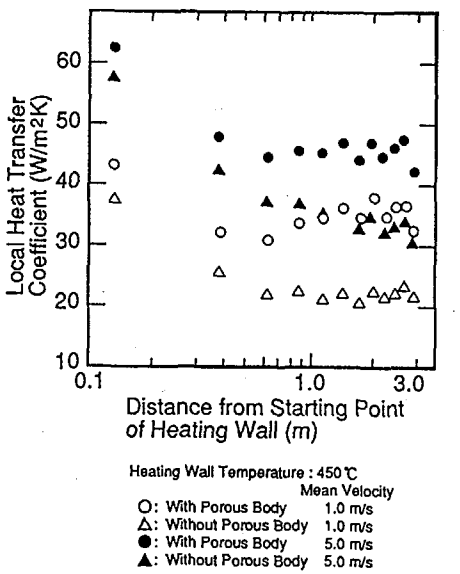

Fig.2 Local heat transfer coefficients.

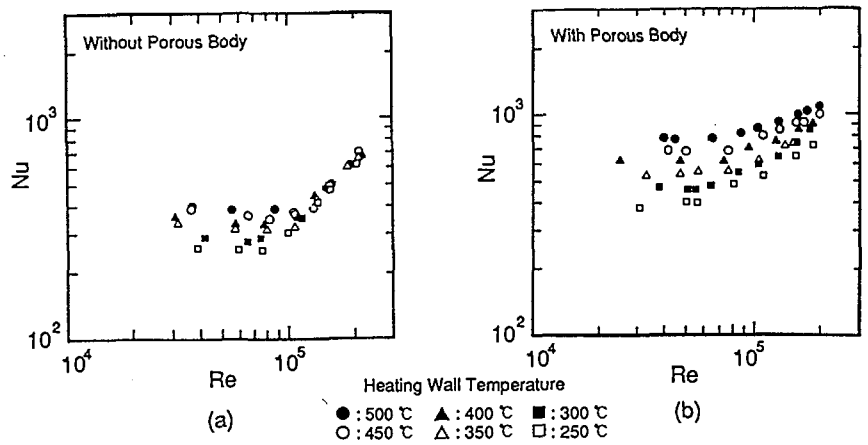

Fig.3 Relation between Nu number and Re number.

Table 1 Heat transfer correlations

Sodium and Reactor Vessel
$Nu = 4.0 + 0.025(Re \cdot Pr)^{0.8}$
Reactor Vessel Conductivity
h =17 W/mK
Emissivity of R/V and C/V
$\epsilon = 0.8$
Containment Vessel Conductivity
h = 45 W/mK
Air flow And Containment Vessel
Fig. 3

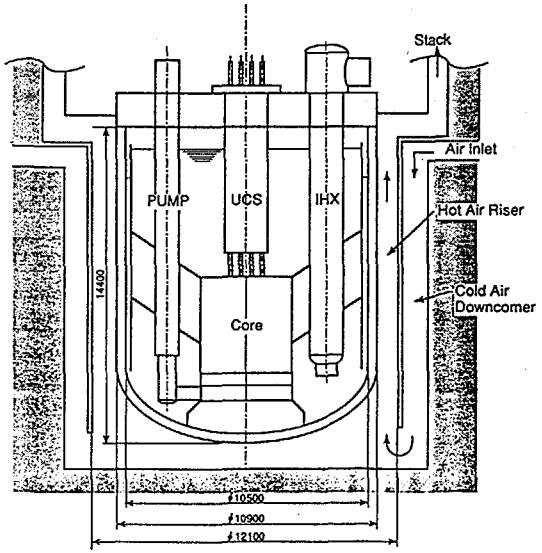

Fig.4 Reference reactor.

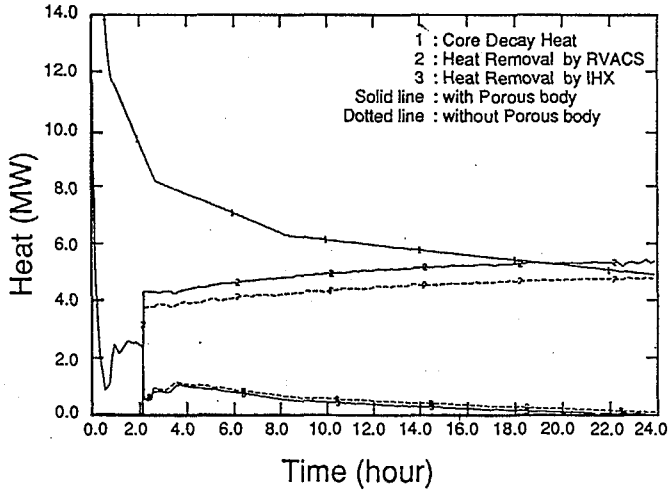

Fig.5 Comparison of core decay heat to heat removal.

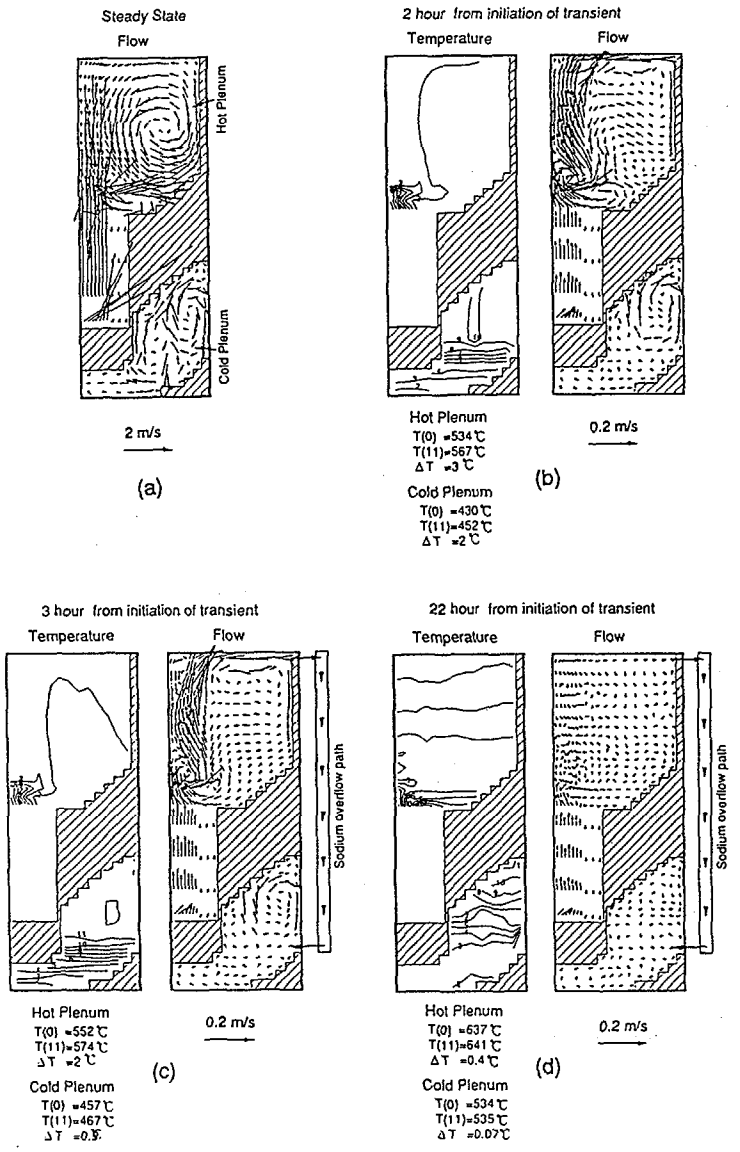

Fig.6 Predicted flow patterns and temperature profiles.

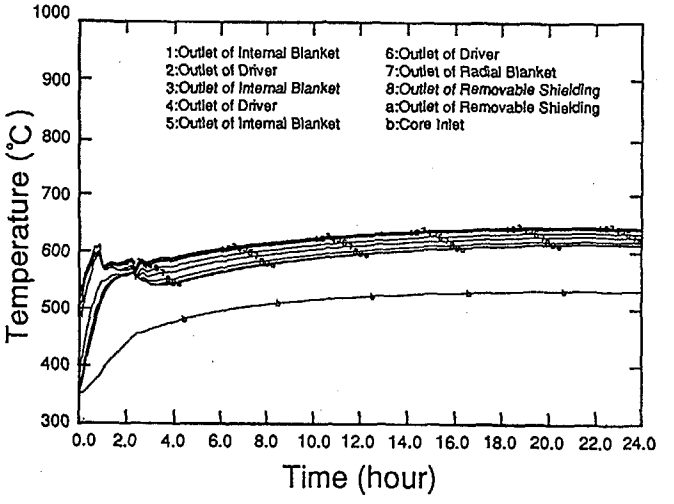

Fig.7 Predicted core outlet temperature.

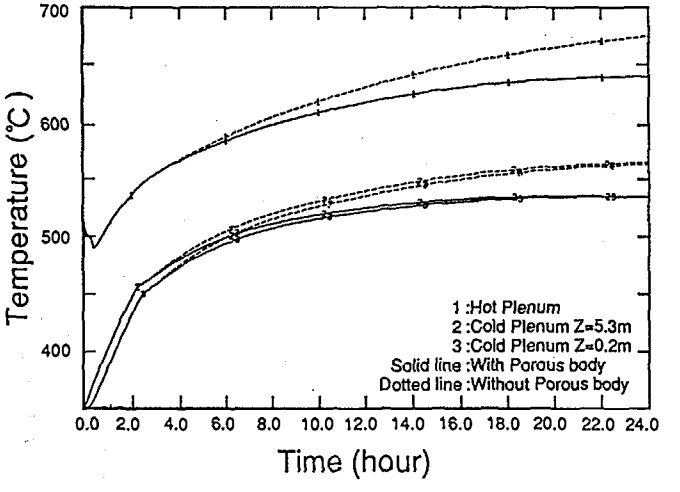

Fig.8 Predicted sodium temperature during transient.

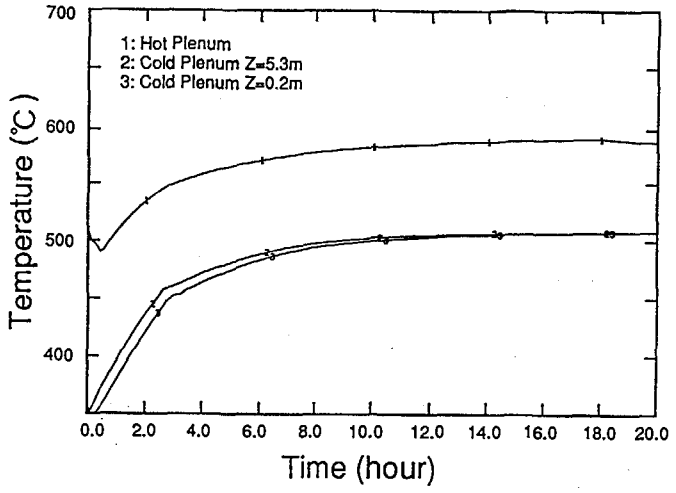

Fig.9 Predicted sodium temperature during transient.
(Reactor vessel diameter is 11m)

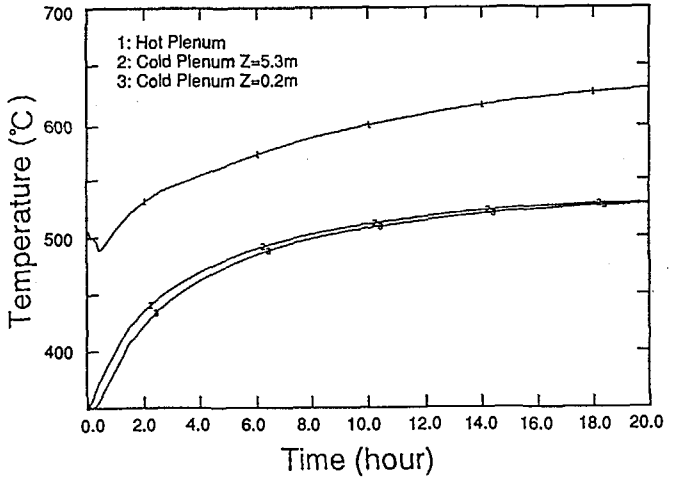

Fig.10 Predicted sodium temperature during transient.
(Overflow level is 10cm)

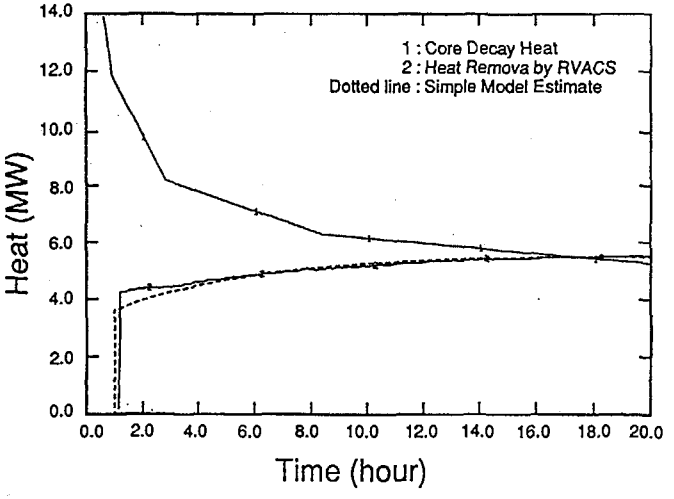

Fig.11 Comparison of core decay heat to heat removal.

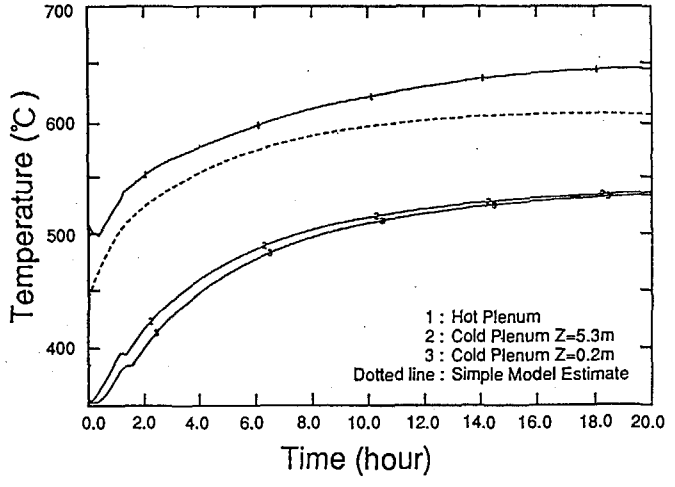

Fig.12 Predicted sodium temperature during transient.

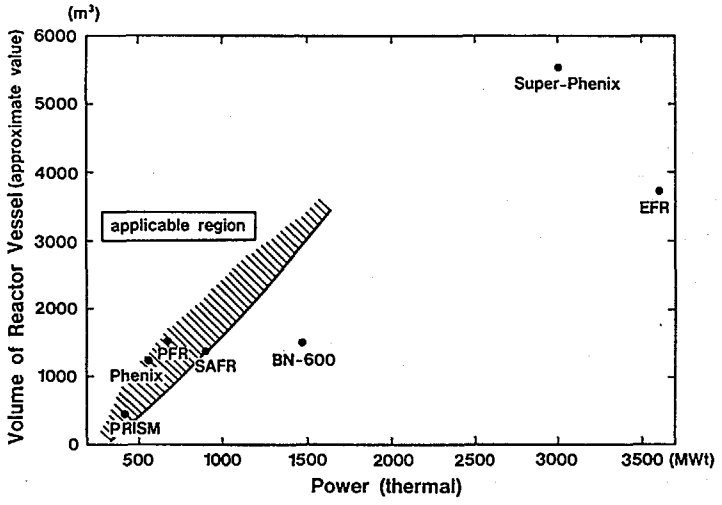

Fig.13 Application limit of this type RVACS.